

Original Research Article

The impact of freshening over the Antarctic Ocean on Pacific Decadal Oscillation

Xiaolin Zhang

Department of Earth and Planetary Sciences, Kyushu University, 744 Motooka, Nishiku, Fukuoka 819-0395, Japan;
xz12j@my.fsu.edu

Abstract: The profound influence of the Antarctic Ocean freshening on the Pacific Decadal Oscillation (PDO) is investigated in this study by utilizing a series of fully coupled ocean-atmosphere 400-year-modeling experiments. The simulated results derived from the Fast Ocean-Atmosphere Model (FOAM) can reasonably identify the spatial pattern and time period (10–20 years and 20–50 years) of the observed PDO with slightly weak amplitudes. In the sensitivity experiment (Southern Ocean Water Hosing), 1.0 Sv (Sverdrup, $1\text{ Sv} = 1.0 \times 10^6 \text{ m}^3/\text{s}$) freshwater flux is uniformly imposed over the Antarctic Ocean for 400 years. As a response to this Antarctic Ocean freshening, the Tropical Pacific Ocean displays a normal “La Niña pattern”, while the low-frequency variability within the North Pacific Ocean is much weakened. Preserving the PDO’s spatial pattern, the multidecadal (20–50 years) magnitude becomes weak and shifts toward higher frequency. In contrast, the decadal magnitude of the PDO (10–20 years) is slightly reinforced and also shifts towards higher frequency. Dynamical analysis indicates that the shortening of the PDO multidecadal variability is mainly caused by the acceleration of the first-baroclinic-mode Rossby waves. The spreading of the fresh anomalies and associated increasing stratification in the North Pacific Ocean result in the shortening of the long Rossby wave propagation to cross the subtropical North Pacific basin. A heat budget analysis further shows that the upper-ocean thermodynamic variability in relationship to the stratification oscillation in the North Pacific Ocean is mainly associated with the anomalous behaviors of the meridional advection, heat flux and ocean mixing.

Keywords: Pacific Decadal Oscillation; freshwater; Antarctica; Rossby waves; heat budgets; coupled models

1. Introduction

Freshwater flux in the Southern Ocean (SO) is an important forcing of the high-latitude ocean and global climate system. In the evolution of the paleoclimate, there have been several glacier ice-melting Melt-Water-Pulse (MWP) events associated with ice sheets in the Antarctic, during which enormous freshwater discharged into the SO in a short time, which led to significant elevating of the sea level and a series of paleoclimate anomalous events^[1,2].

In recent decades, as global warming intensifies, the potential impacts of freshwater flux over the SO have drawn much more attention. Studies showed that several Antarctic ice shelves appeared to break up suddenly under global warming, such as the great ice-melting of the Larsen A shelf, Wilkin shelf and Larsen B shelf^[3]. Rignot et al.^[4] further found that large areas of the West Antarctic have suffered great glacier ice-melting and the Antarctic melting is significantly intensified in present-day^[5,6]. For example, ice sheet loss in the Amundsen Sea and Bellingshausen Sea has increased by 59% within 10 years, and the loss rate in 2006 even reached $132 \pm 20\text{ Gt}/\text{year}$ ^[4]. The ice melting in the Antarctic that is triggered by global warming has been one of the most serious climate events. Once large-scale ice-melting in the Antarctic happened, there would be an enormous amount of freshwater discharged into the SO, the impact of which on the global climate system drew great interest from climatologists. For example, the Antarctic Ice Sheet Melt has been shown to impact the location of the Intertropical Convergence Zone (ITCZ, Hadley cell, atmospheric bridge), and the global climate through the oceanic and atmospheric bridges and associated local sea surface salinity (SSS), sea surface

temperature (SST) and atmosphere-ocean feedback^[7–11].

Pacific Decadal Oscillation (PDO) is the strongest natural decadal climate variation in the North Pacific Ocean^[12]. Generally, the first Empirical Orthogonal Function (EOF) mode of the North Pacific (north of 20°N) SST anomaly is defined as the PDO mode with its principal component as the PDO index. Mantua et al.^[13] utilized the time series of the North Pacific SST pattern as the indicator of polarity and showed that during the 20th century, the PDO was predominantly positive between 1925 and 1946, negative between 1947 and 1976, and positive since 1977. Minobe^[14] further found that the PDO presents two significant periods of 15–25 years and 50–70 years, respectively. Both the observation and the ocean model results indicate that the PDO pattern in the North Pacific Ocean corresponds to a specific atmosphere forcing field, which is called Aleutian Low (AL) anomaly forcing^[12,15]. In the high altitude, associated with the AL pattern is the Pacific-North America (PNA) pattern atmospheric teleconnection wave train^[16], so the AL pattern is also called the PNA pattern.

When the PDO is in a warm phase, the SST anomaly in the North Pacific presents a basin-wide horseshoe-like spatial distribution with a cooling in the central and western North Pacific surrounded by cooling to the north, east, and south^[13,17]. Associated with the anomalous patterns of the PDO, a stronger-than-normal AL^[13] is established with its center shifting toward the southeast^[12,18] and lower-than-normal 500-mb geopotential height field^[13]. At the same time, the westerly in the midlatitude will strengthen. When the PDO is in the cold phase, the situation is opposite to the above results^[18,19]. Recent studies showed that PDO has an impact on climate variability in various regions^[20–22].

Various views are proposed on the mechanism of the PDO^[23] (see **Table 1**). Gu and Philander^[24] owed the origin of the PDO to the entire extratropical-tropical climate systems, which are related to each other by atmospheric or ocean teleconnection. Latif and Barnett^[25,26] suggested that the PDO arises from the coupled ocean-atmosphere system over the North Pacific and the ocean Rossby wave plays an important role. Recent studies indicated that the global climate system is suffering from prominent changes under global warming, which has an important influence on the generation of PDO. Fang^[27] pointed out that the PDO would be weakened and shift to higher frequency as a result of the ocean Rossby wave speed change under global warming. Rashid et al.^[28] found that freshening over the North Atlantic Ocean would weaken the AMOC and then strengthen the PDO, at the same time the cold phase of the PDO would occur more frequently. New developments in PDO have been made by recent research^[29–32].

Table 1. Theoretical frameworks of North Pacific decadal variations.

Theoretical frameworks	Authors	The hypotheses
Stochastic atmospheric forcing mechanism	Frankignoul and Hasselmann ^[33] ; Alexander and Penland ^[34] ; Jin ^[35] ; Pierce et al. ^[36]	SST decadal variability arises from oceanic integrating effects on large-scale atmospheric stochastic forcing.
The midlatitude ocean-atmosphere feedback mechanism	Latif and Barnett ^[25,26]	Ocean-atmosphere coupling over the midlatitudes serves as a candidate mechanism for the decadal variability of the PDO.
Tropical-extratropics mechanism	Trenberth and Hurrell ^[12] ; Gu and Philander ^[24] ; Jacobs et al. ^[37] ; Graham ^[38] ; Alexander et al. ^[39]	PDO could have originated in the tropical Pacific and then influenced the mid-latitude by atmospheric or oceanic teleconnections to midlatitudes.
Ocean dynamics mechanism	Latif and Barnett ^[25,26] ; Miller et al. ^[40]	The oceanic Rossby wave driven by the atmospheric forcing plays a crucial role in maintaining and setting the time scale of PDO decadal variability.
Advective resonance mechanism	Saravanan and McWilliams ^[41]	The advective resonance mechanism generates decadal SST variability in the Eastern North Pacific associated with the anomalous Ekman advection and surface heat flux.
Intrinsic ocean variability mechanism	Holland and Haidvogel ^[42]	Intrinsic nonlinear variability of western boundary current systems with steady wind forcing may produce decadal variations that rely on the eddy effects in the recirculation zone.

Freshwater flux over the SO, which once led to the MWP events during the last deglaciation and is the important product of the Antarctic ice melting induced by global warming, has a potential impact on global climate and associated PDO variability. Consequently, in the previous work associated with climatic impacts of SO freshwater injection, mean-climate change has been well investigated, but the discussion of modulation of climatic mode including the Southern Annular Mode (SAM) and PDO remains elusive. In fact, although the study of teleconnection between the Southern and tropics as well as the Northern Hemisphere is abundant^[35,43–55], the quantitative impact of the SO freshwater forcing on the PDO is still lacking in investigation. In this study, we will explore the influence of freshening over the Antarctic Ocean on the PDO variability.

The paper is organized as follows. A brief description of the model and data is provided in Section 2. Sections 3 and 4 describe the model simulated PDO in the CTRL and SOWH experiment. Section 5 demonstrates the potential mechanisms responsible for the changes of the PDO on freshening over the Antarctic Ocean. Concluding remarks and further discussion are provided in Section 6.

2. Materials and methods

In this study, we used a fully coupled ocean-atmosphere general circulation model, Fast Ocean-Atmosphere Model, version 1.5 (FOAM1.5)^[56], which is developed jointly at the University of Wisconsin-Madison and the Argonne National Laboratory. The atmospheric component of FOAM is a fully parallel version of the National Center for Atmospheric Research (NCAR) community climate model version 2 (CCM2), which has an R15 resolution, but with a vertical resolution of 18 levels and the atmospheric physics replaced by those of CCM3. The ocean model is conceptually similar to the second version of the Geophysical Fluid Dynamics Laboratory (GFDL) Modular Ocean Model (MOM), with a resolution of 1.4° -latitude \times 2.8° -longitude \times 32-level, and is designed for massively parallel platforms. With a simple thermodynamic sea ice model is incorporated, the fully coupled model has been integrated for over 2000 years without apparent climate shift.

FOAM not only reasonably captures the features of the observed climatology^[56], but also reproduces the main climate variability patterns in different oceans, such as ENSO^[57], North Pacific decadal climate variability^[19,58], North Atlantic Oscillation (NAO) and North Atlantic decadal climate variability^[59]. As a whole, the climate variability patterns simulated by FOAM basically coincide with what we get from the observation. However, it should be noted that the version used in this study is basically the same as that used by Wu and Liu^[59], but with the vertical resolution of the ocean model increased from 24 to 32 levels and some other changes in the sea-ice and land model components.

We analyzed the impact of freshening over the Antarctic Ocean on PDO through four datasets: FOAM1.5 Control run (CTRL) data, Southern Ocean Water-Hosing (SOWH) data, Hadley Centre Global Sea Ice and Sea Surface Temperature dataset (HadISST)^[60] data and NCAR/NCEP data.

In the SOWH experiment, 1.0 Sv (Sverdrup, $1 \text{ Sv} = 1.0 \times 10^6 \text{ m}^3/\text{s}$) freshwater flux was added uniformly to the south of 60°S (the intensity of freshwater forcing is equal to a local sea level rise of about 155 cm/year) as a virtual salt flux. This rate was fixed for 700 model years. CTRL experiment was a parallel experiment starting from the same initial condition, which was also conducted for 700 years with no freshwater anomaly added. It should be noted that here the virtual salt flux scheme is relatively simple and the freshwater flux changes the salinity of the seawater parcel by changing its salt content while keeping its volume constant. This will introduce biases in regions where the SSS largely differs from the reference salinity^[61]. A more realistic treatment should consider the effect of Freshwater flux (FWF) on the vertical velocity, oceanic temperature, and surface buoyancy flux as pointed out by Griffies et al.^[62] and Kang et al.^[63], which will be an interesting topic for our future work.

The differences between these two experiments were taken as the modeling responses. In order to make the results more reliable, the last 400-year data when the model reached the steady state was used for the analysis in this study.

To provide a reference for the model variability, we compared the model PDO with the observed PDO. The monthly mean observational SST data used in this study is from the HadISST. It consists of data from 1870 to 2007 with a resolution of 1.0° latitude × 1.0° longitude. The monthly mean geopotential height data is from NCAR/NCEP Reanalysis from 1871 to 2008.

To focus on the decadal timescales, the data have been linearly detrended and low-filtered to retain variability whose period is longer than 10 years before EOF analysis so as to keep the decadal standard deviation. The statistical test used in our study shows that the power spectrum is red noise.

3. Model-simulated PDO

To examine the PDO simulated by the model, we analyzed the observations for a comparison. In the observation (HadISST), the PDO emerges as the first EOF mode of monthly mean SST anomalies over the North Pacific (north of 20°N), which accounts for 24.75% of total variances (**Figure 1(a)**). From the power spectrum, we can find enhanced power around decadal timescales (**Figure 1(c)**). Associated with the PDO mode, the variations of the atmospheric circulation over the North Pacific reveal a monopole pattern, which is

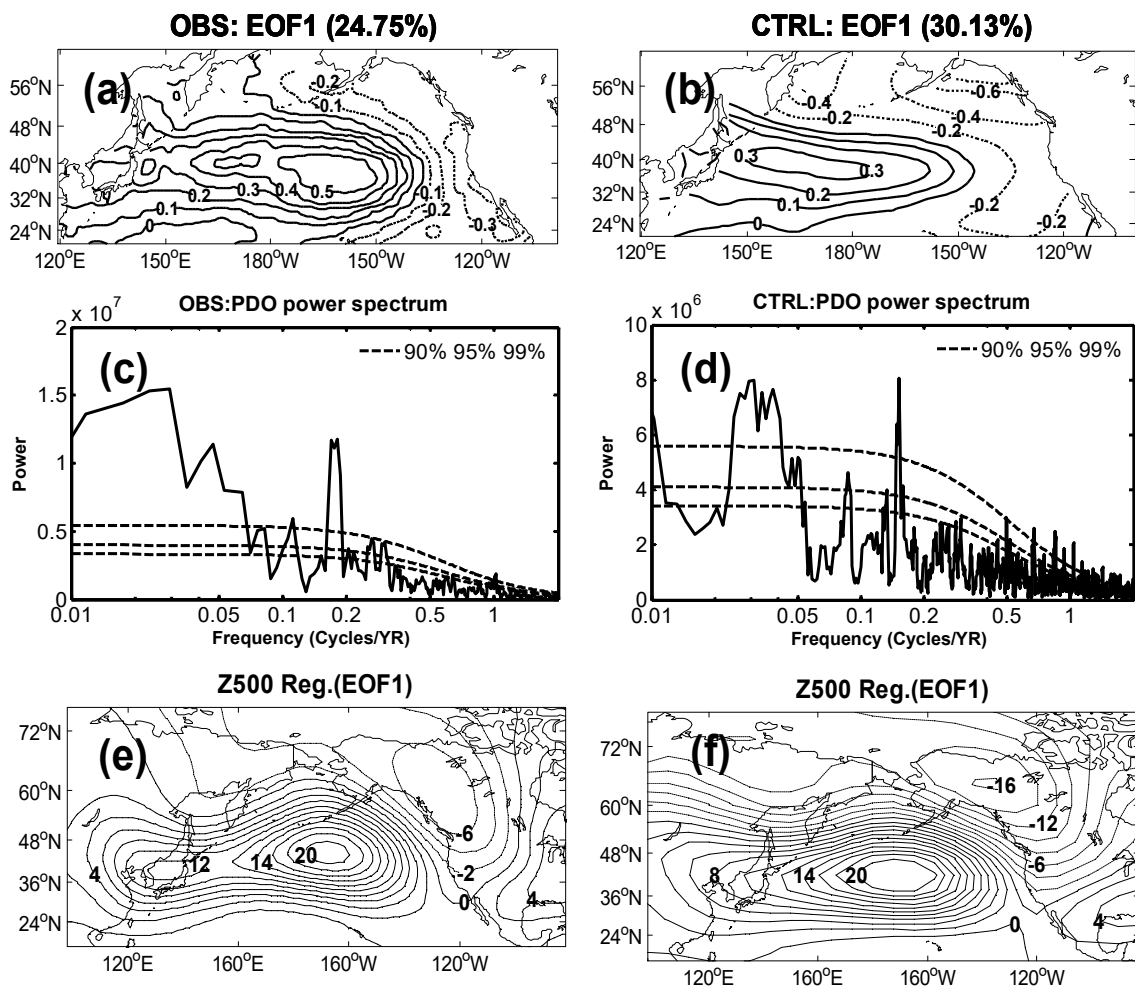


Figure 1. Observed (left panel) and model simulated (right panel) leading modes of North Pacific (north of 20°N) anomalies. ((a), (b)) PDO SST mode, ((c), (d)) power spectrum of PDO time series (principal component of the corresponding EOF mode), and ((e), (f)) Regression of the 500-mb geopotential height anomalies against the principal component. Units for SST EOFs and Z500 regression are °C and gpm, respectively.

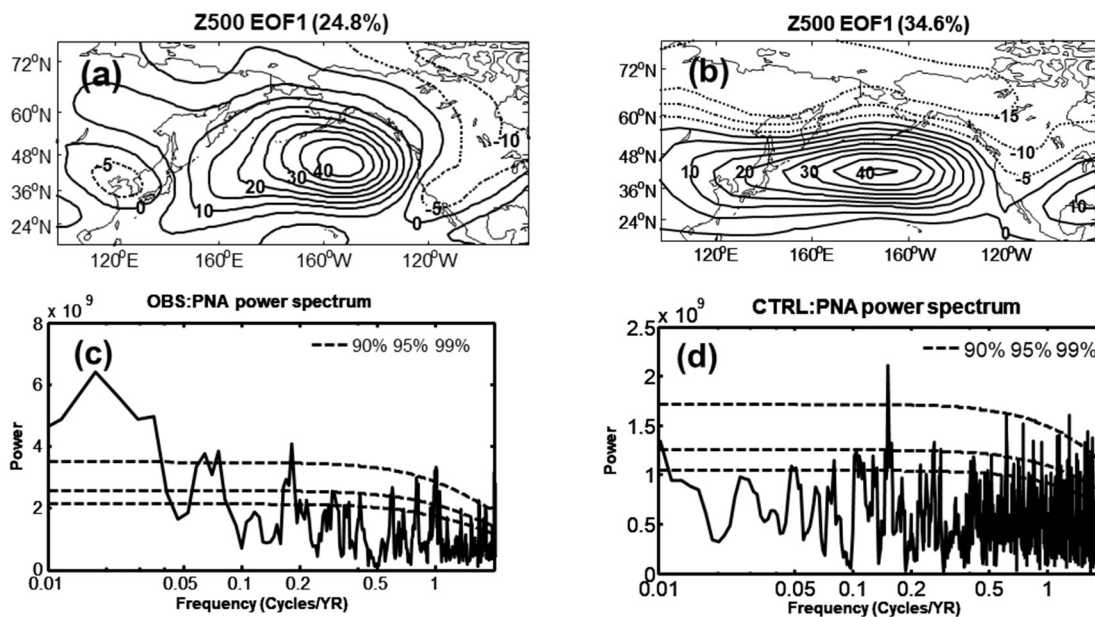


Figure 2. The first EOF mode of (a) observed and (b) model simulated 500-mb geopotential height anomalies. (c) and (d) power spectrum of the time series of the Z500-mb EOF1 in the observation and model. Unit for EOF is gpm.

obtained by regressing the 500-mb geopotential height from the NCEP/NCAR reanalysis against the PDO index (defined as the principal component of the PDO mode) from 1871 to 2007 (Figure 1(e)). This pattern resembles the leading EOF mode of the geopotential height over the North Pacific sector, namely PNA pattern (Figure 2(a)).

As the above-mentioned method in Section 2, we performed EOF analysis on the FOAM1.5 data, too. The simulated PDO pattern in the FOAM CTRL experiment is broadly similar to the observation (Figure 1(b)). However, the PDO pattern in the FOAM1.5 can explain 30.13% of the variance, which is larger than that in the observation. Besides, compared to the observational results, the PDO pattern extends less easterly and northerly and the center of the maximum somewhat shifts towards the northwest in the FOAM 1.5. In addition, the amplitude of the PDO mode is stronger in the observation, which can reach 0.5 °C. However, the simulated PDO displays notable spectral peaks around 10–20 years and 20–50 years (Figure 1(d)). Overall, FOAM1.5 can capture the main features of the PDO mode although it is weaker than that in the observation.

Compared with the observation, the regression of 500-mb geopotential height against the PDO index exhibits a similar pattern (Figure 1(f)). In the model, a PDO with a warming in the central and western North Pacific, which is surrounded by cooling to the north, east, and south, is associated with a weaker-than-normal AL resembling the leading EOF mode of the 500-mb geopotential height in the model (Figure 2(b)).

4. PDO variability under freshening over the Antarctic Ocean

4.1. Mean state

Freshwater forcing over the SO triggers a regional coupled response of ocean-atmosphere-sea ice. The freshening leads to a strong regional cooling, accompanied by the intensification of local westerlies, and northward extension of sea ice margin. Such cooling is largely trapped in the upper 50 m with substantial warming underneath, inhibiting deep convection and the formation of Antarctic Bottom Water^[64].

Over the tropical Pacific, the spatial structure of the mean SST response shows a “La Niña-like” pattern, which exhibits warming in the western tropical Pacific and cooling in the east (Figure 3(a)). It has been demonstrated that tropical SST response in the Pacific panel was originated both air-sea coupled pathways in the Southern Hemisphere^[64]. Meanwhile, the tropical thermocline becomes sharper, which is associated with

enlarged interannual standard deviation in tropical Pacific and strengthened ENSO variability^[64].

Over the North Pacific, the mean SST response displays a general warming pattern, but with significant regional differences (**Figure 3(a)**). The maximum SST increase appears in the western subpolar Pacific, which can reach up to 1.1 °C. The warming signal can extend to northeast of the subtropical Pacific. The general warming of the North Pacific may be associated with freshening over the Antarctic Ocean through deep subduction, which has been indicated in the study of Ma and Wu^[64]. In response to freshening over the Antarctic Ocean, the local subsurface reveals warm anomaly, which will reach the midlatitude of the North Pacific through a slow subductive process and then enter into the mixing layer by vertical mixing process. As a result of the above processes, the upper ocean in North Pacific reveals warm anomaly (**Figure 3(b)**) and the warming increases with the depth. Besides, this warming may be related to the slowdown of the Subtropical Cell (STC), which is able to induce less heat transmission from the tropics and cause less northward transport of the relatively cold deep water in the subsurface (not shown). In addition, the water becomes fresher at the the same time, the maximum fresh anomaly appears on the surface of the subtropical North Pacific, which can reach up to -1.5 psu and the anomaly decreases with the increasing depth in most regions (**Figure 3(c)**). The anomaly of the salinity is likely associated with the advection of the freshwater flux, which is due to freshening over the Antarctic Ocean. Freshening over the Antarctic also exerts remarkable impacts on winds. In response to freshening over the Antarctic Ocean, there forms an easterly anomaly over 40°N–60°N, implying a weakening and southward shift of the mean westerly, which may contribute to an intensification of local warm anomaly (**Figure 3(d)**).

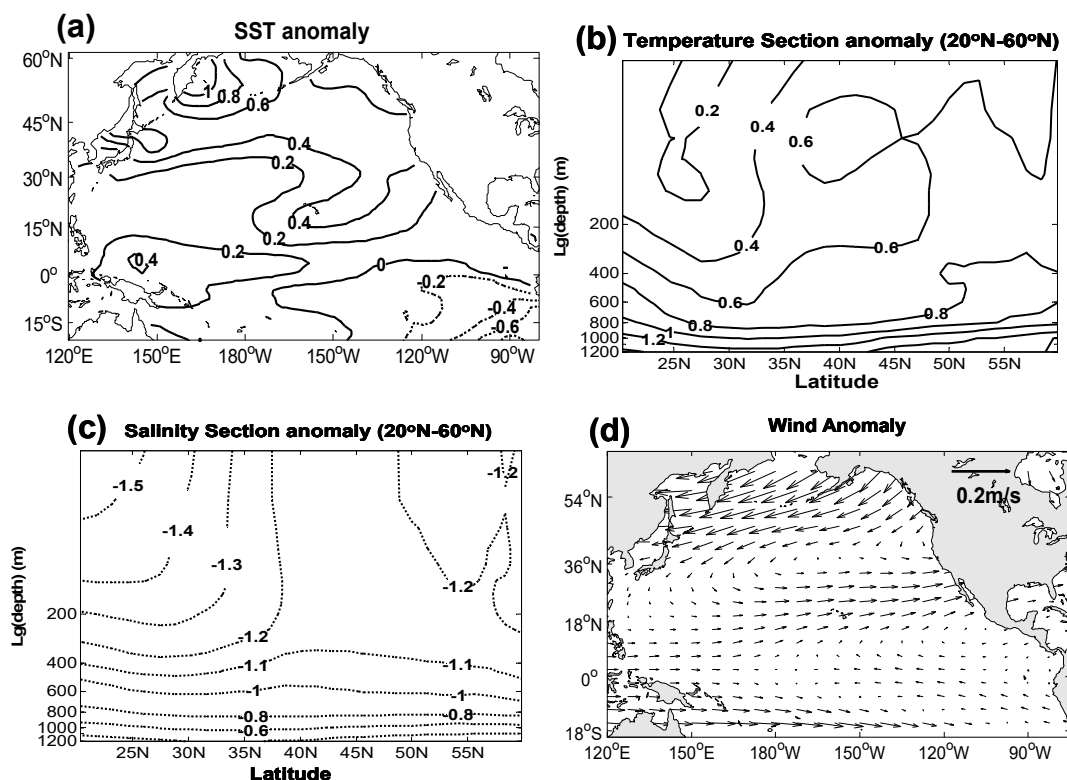


Figure 3. Anomalies (SOWH minus CTRL) of (a) SST, depth-latitude section of (b) temperature and (c) salinity over the North Pacific (20°N–60°N), and (d) surface wind. Units for temperature, salinity and wind are °C, psu and m/s, respectively.

4.1. PDO

In response to freshening over the Antarctic Ocean, the decadal standard deviation of North Pacific SST displays a negative anomaly and the maximal value emerges in the western subpolar Pacific, which is about

-0.15 °C. When the entire basin is concerned, the SST decadal standard deviation appears negative anomaly (**Figure 4(a), (b)**). In a word, the decadal variability of the North Pacific is weakened as a result of freshening over the Antarctic Ocean. The changes of the 500-mb geopotential decadal standard deviation also reveal a negative anomaly, which is consistent with the results of the SST in the North Pacific (**Figure 4(c), (d)**).

To investigate the impact of freshening over the Antarctic Ocean on the PDO pattern, we conducted an EOF analysis on North Pacific SST anomaly in the SOWH. The first EOF mode of the SST anomalies in the SOWH experiment shows the PDO pattern resembling that in the CTRL experiment (**Figure 5(a)**). The mode explains about 27.60% of the total variance and exhibits a well-defined horseshoe-like spatial pattern. The regression of 500-mb geopotential height against the PDO index also displays a PNA-like pattern similar to that in the CTRL experiment (not shown), suggesting that the PDO-PNA coupled pattern preserves when freshening over the Antarctic Ocean.

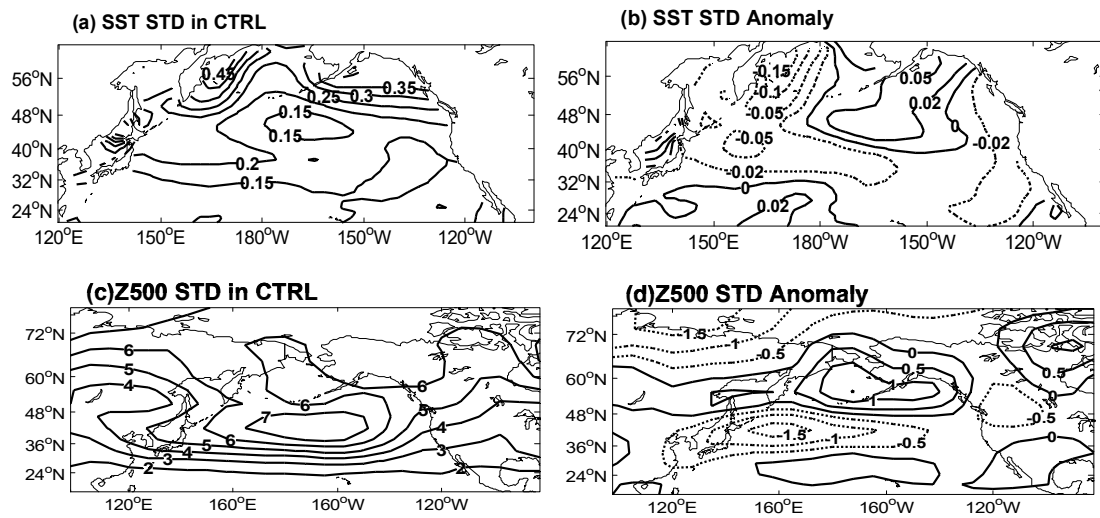


Figure 4. Decadal standard deviation of Pacific SST and Z500 (a 10-year low-pass filter is used) (units: °C and gpm). (a) and (c) for CTRL experiment, while (b) and (d) for difference between SOWH and CTRL.

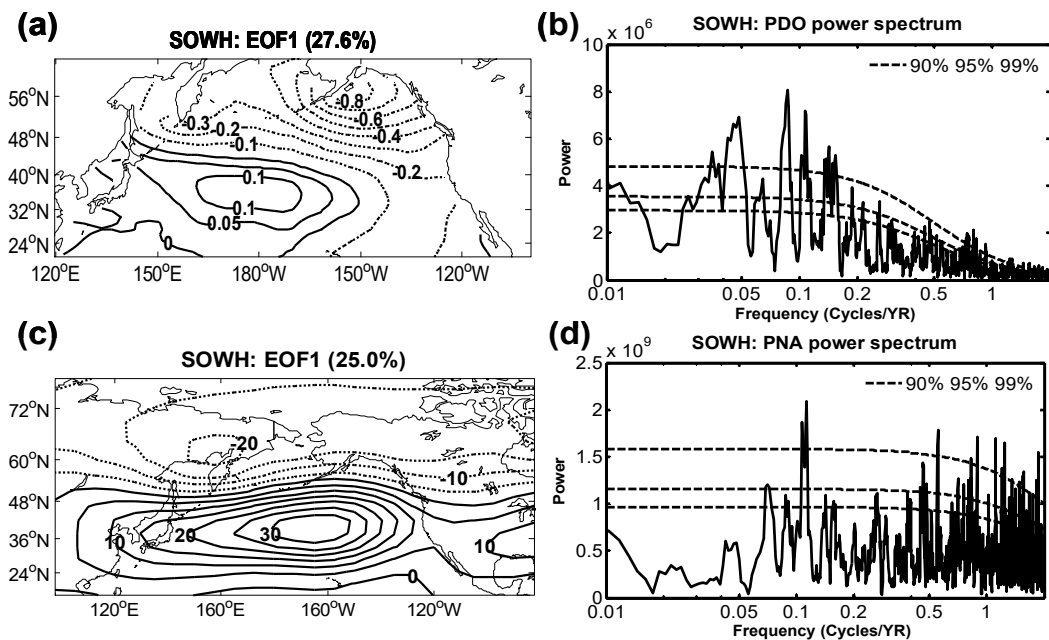


Figure 5. Leading EOF of (a) SST and (c) Z500 anomalies in SOWH experiment. Power spectrum of PC1 for (b) SST and (d) Z500. Units for SST and Z500 EOFs are °C and gpm, respectively.

The most striking changes of the PDO-PNA mode occur in their temporal evolution. In the SOWH experiment, the 20–50 year magnitude of the PDO is weakened and shifts toward higher frequency, however, the magnitudes of the 10–20 years variability are slightly reinforced (**Figures 1(b) and 5(b)**)^[65]. Herein, we draw a preliminary conclusion that the multidecadal variability of the PDO is weakened due to the enhanced freshwater flux over the Antarctic Ocean. The enhancement of interdecadal variability (10–20 years) seem to be associated with tropical teleconnections, which will be briefly discussed in Section 5.3.

5. Mechanisms

5.1. Heat balance

To understand the mechanism controlling the generation of the SST decadal oscillation in the North Pacific Ocean, a heat budget analysis is utilized for the CTRL run. All of the data have been band passed to retain the variability between the 20 and 50 years. Note here and in the following sections, traditional ways are used to explore the possible dynamics related to the response of PDO to freshening over the Antarctic Ocean. More advanced methods will be used to confirm the robustness of our conclusions in future work. The details of the heat budget equation are:

$$\frac{\partial T}{\partial t} = -u \frac{\partial T}{\partial x} - v \frac{\partial T}{\partial y} - w \frac{\partial T}{\partial z} + \frac{Q}{\rho_0 C_p H} + R \quad (1)$$

where T is the temperature, u , v , and w are the zonal, meridional and vertical velocity, respectively. Q is the surface flux, ρ_0 is the seawater density, C_p is the specific heat, H is the mixing depth (used upper 100 m here) and R is the residual terms (representing the diffusion and convection processes). The advection terms can further separate into anomalous current advection ($u'T_x$, $v'T_y$, and $w'T_z$), and mean advection (UT'_x , VT'_y , and WT'_z). The anomalous current (u' , v' , and w') is defined as the deviation from the climatological mean current (U , V , and W). Here all of these terms are vertically averaged over the upper 100 m to focus on the upper layer thermodynamic processes.

The instantaneous regression of all these terms is displayed in **Figure 6**. In addition, we also calculated the regression of SST and wind stress. The heat budget analysis reveals that the PDO is primarily associated with the anomalous meridional advection (**Figure 6(f)**), heat flux (**Figure 6(i)**) and ocean mixing (**Figure 6(j)**). Specifically, in the center and western North Pacific, warm (cold) anomalies are created predominantly by the anomalous meridional advection (**Figure 6(f)**) in response to the anomalous easterlies (westerlies), which will bring warm (cold) water from lower (higher) latitudes (**Figure 6(b)**) and the heat flux will strengthen the warm (cold) SST anomalies in most regions, however, the convection and ocean mixing will damp the SST anomalies. We should pay attention to the western boundary currents region, where the SST anomalies will be damped by the heat flux (**Figure 6(i)**), mean zonal advection (**Figure 6(c)**) and mean meridional advection (**Figure 6(e)**), however, will be strengthened by the convection and ocean mixing (**Figure 6(j)**). In the subpolar Pacific, cold (warm) SST anomalies are primarily created by anomalous zonal (**Figure 6(d)**) and meridional (**Figure 6(f)**) advection and are damped by the heat flux in the western and strengthened in the eastern.

In summary, the analysis of the upper-ocean heat budget reveals a dominant role of the anomalous meridional advection, heat flux and ocean mixing in the generation of decadal SST anomalies over the North Pacific.

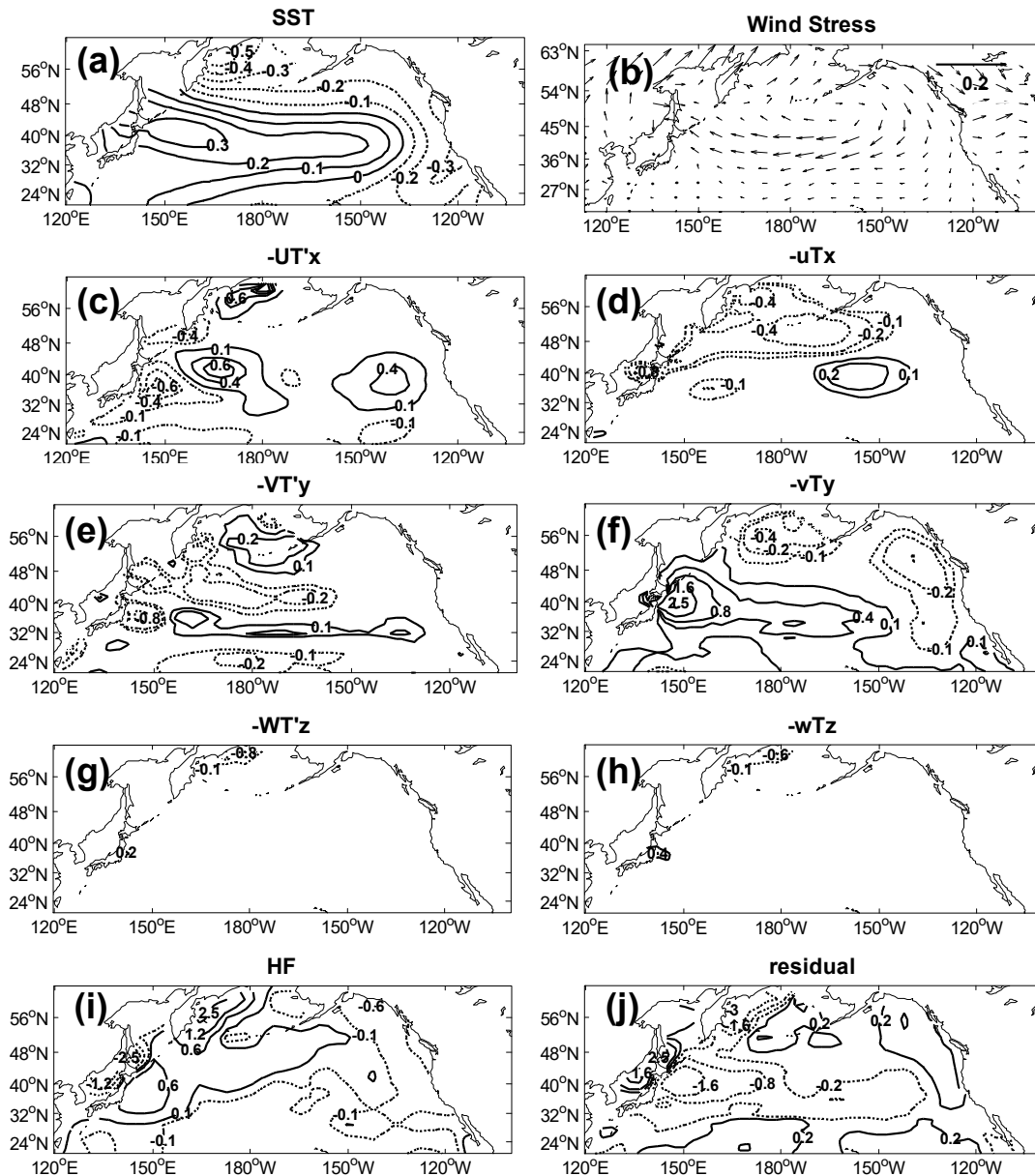


Figure 6. Regression of (a) SST, (b) wind stress, (c) anomalous and (d) mean zonal advection, (e) anomalous and (f) mean meridional advection, (g) anomalous and (h) mean vertical advection, (i) surface heat flux (positive downward), and (j) residual on the PDO index. All data are band passed to retain the variability between 20 year and 50year. Units for SST, wind stress and heat balance terms are $^{\circ}\text{C}$, Nm^{-2} and Wm^{-2} ($\times 10^{-8}$) per standard deviation of the index, respectively. The vertical parts are $^{\circ}\text{C}$ ($\times 10^{-13}$) per standard deviation of the index.

5.2. Modulation of Rossby wave dynamics by freshening over the Antarctic Ocean

One important oceanic change in freshening over the Antarctic Ocean is the stratification. Because the warm anomalies over the North Pacific is from the local subsurface warming in the Antarctic Ocean, which influences the North Pacific upper ocean through a slow subductive process, the subsurface ocean warms faster than the surface in the North Pacific, leading to a weakening oceanic stratification. Our previous modeling study shows that the subsurface warm water in the North Pacific Ocean is from the Southern Ocean. Local freshwater forcing is able to strengthen oceanic stratification in the Antarctic region and triggers surface cooling and subsurface warming, and then the subsurface warm signal can be transmitted to the North Pacific through a slow subductive process.

The salinity reveals negative anomaly in the North Pacific, which decreases with increasing depth. Due

to the combinative effect of temperature and salinity, the Brunt Vaisala Frequency displays positive anomaly except in the upper ocean in the north of 30°N and the positive anomaly increases with the depth (Figure 7(b)), which finally leads to an increase in the stratification. From the zonal mean density anomalies in the North Pacific, we can draw the same conclusions (Figure 7(a)).

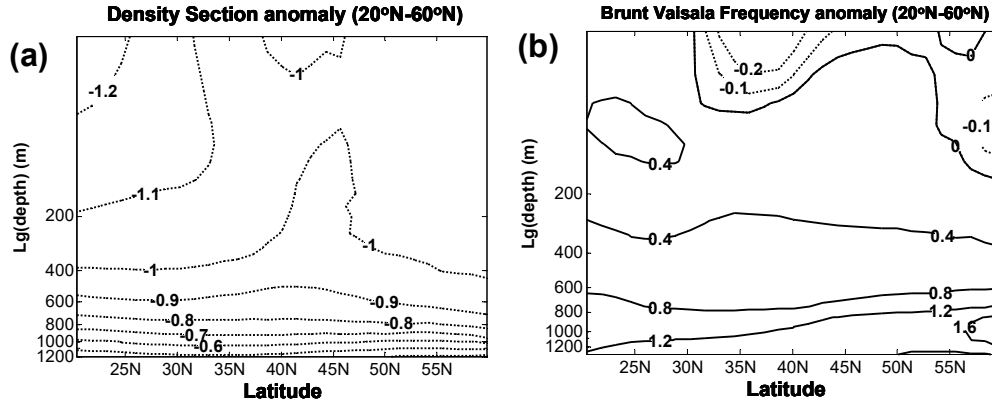


Figure 7. Zonal mean (140°E–110°W, 20°N–60°N). (a) density and (b) Brunt Vaisala Frequency anomalies (SOWH minus CTRL) of North Pacific (units: kg/m³ and 10⁻³/s).

Following Chelton et al.^[66] and Yang et al.^[65], the speed of the *n*-order baroclinic Rossby wave in the north of 5°N is:

$$C_{R,n} \approx -\beta L_{R,n}^2 = -\beta \left(\frac{1}{n\pi|f|} \int_{-H}^0 N(z) dz \right)^2 \tag{2}$$

where $L_{R,n}$ is the Rossby radius of deformation, *n* is the order of the baroclinic Rossby wave, *f* is the Coriolis parameter, β is the meridional gradient of *f*, and *N*(*z*) is the buoyancy frequency.

By taking account of the mean flow ($\frac{\partial u(z)}{\partial z}$), the speed of the baroclinic Rossby wave can be calculated as follows:

$$(u - c)W_{ZZ} - u_z W_z + \frac{\beta N^2}{f^2} W = 0 \tag{3}$$

where *W* is the characteristic function of vertical velocity. By taking the vertical finite difference for Equation (3), we can get: $AW = cBW$, *A* and *B* are matrices, then we can calculate the eigenvalue *c* and the eigenvectors *W*. From Equations (2) and (3), we can conclude that the Rossby wave speed depends on latitude and the ocean stratification. More specifically, the Rossby speed decreases as the latitude increases (the ocean stratification reduces).

The first-mode baroclinic Rossby wave in the CTRL run and SOWH run are shown in Figure 8. As we expected, the zonal distribution of the Rossby wave speed derived from the CTRL run is faster when it is closer to the equator than that of the SOWH run. In response to freshwater flux into the Antarctic Ocean, the speed of the first-mode baroclinic Rossby wave increases in the North Pacific Ocean. The maximal value appears in the subtropical North Pacific, which can reach up to 6 cm/s. In addition, the maximal value of the variation ratio appears in the eastern Pacific, which is about 60% and decreases westwards. Although other factors such as large-scale tropical waves may also work, given the important role of the subtropical Rossby wave in setting up the timescales of the PDO decadal variability, the acceleration of Rossby wave in the subtropics by freshening over the Antarctic Ocean, therefore, leads to a shortage of decadal memory in the subtropical ocean. An increase of 60% in the first-mode baroclinic Rossby wave speed may lead to a reduction of the cycle from 30-year to about 20-year, consistent with the frequency shift of the PDO spectrum (Figure 5(b)).

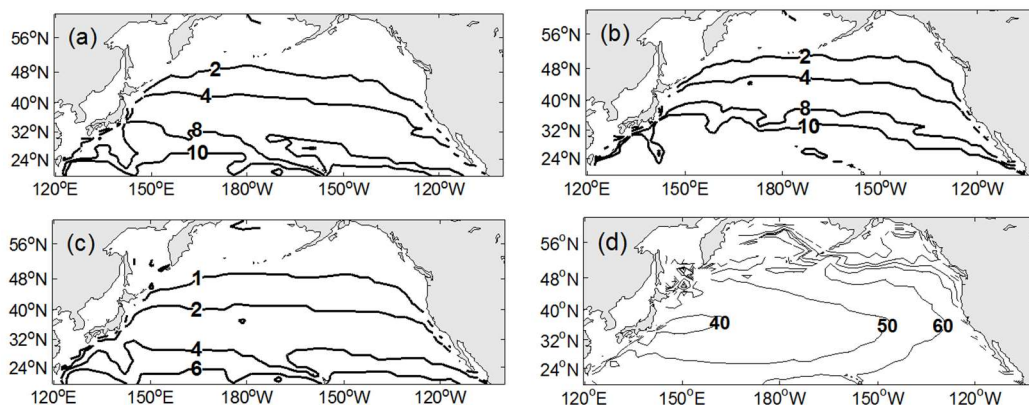


Figure 8. The first-mode baroclinic Rossby wave speed (with consideration of the mean flow) (units: cm/s). **(a)** CTRL; **(b)** SOWH; **(c)** difference between SOWH and CTRL experiment; **(d)** variation ratio (wave speed differences divided by that of CTRL).

In short, the acceleration of the first-mode baroclinic Rossby wave as a result of the reinforcement of the ocean stratification is the main reason of the suppression of PDO (20–50 year period).

5.3. Role of tropical atmospheric bridge

Although Rossby wave dynamics have been demonstrated important for the adjustment of PDO variability, so far, the role of tropical atmospheric teleconnection has not been discussed. As the source region of ENSO, tropical teleconnection is the most distinct over the global ocean^[67], and many studies propose that PDO could originate in the tropical Pacific and then influence the mid-latitude by atmospheric tunnel^[12,37,38].

To clarify the role of the tropical Pacific atmospheric bridge, the result of a “partial coupling” (PC) experiment is analyzed, and in this experiment, tropical SSTs are replaced by climatological values to drive the atmospheric circulation above so air-sea coupling is deactivated in the global tropics (10°S–10°N); in this way, the atmospheric teleconnection from the tropics to the extratropics is turned off. To prevent the model climatology drift due to the PC strategy, a parallel experiment is also carried out with no freshwater forcing added over the Antarctic to configure as the corresponding PC control run. The PC experiment explicitly shows that without air-sea coupling in the tropics, warming of the North Pacific is significantly weakened (**Figure 9**), which readily suggests that the tropical SST does play a role in the formation of the North Pacific warm anomaly. This is also consistent with the work by Ma and Wu^[64].

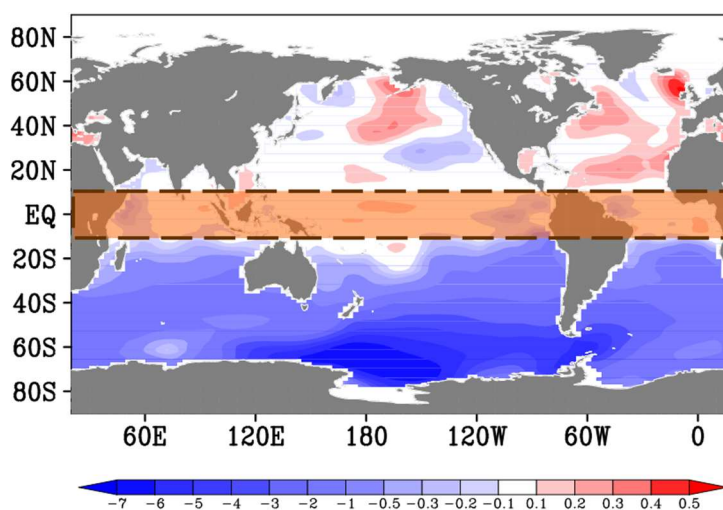


Figure 9. SST (°C) response in tropical PC experiment. red and blue shaded areas denote positive and negative values, respectively. Values over the shaded regions exceed the 95% statistical significance level using a *t*-test. The orange box with dashed thick margin stands for the PC domain^[64].

Besides, when tropical air-sea coupling is removed, typical spatial distribution of the PDO pattern (the first EOF mode) is also eliminated. The spectrum for PC1 only displays a strong peak in the 10–20 year range, which may indicate the important role of tropical Pacific air-sea coupled pathway in modulating the 10–20-year variability in North Pacific (not shown). With the modeling-surgery technology, it can be demonstrated that tropical air-sea coupling does play a potential role in modulating PDO variability.

6. Conclusion

In this paper, the impacts of freshening over the Antarctic Ocean on PDO are studied by conducting a series of coupled ocean-atmosphere experiments. Compared with the observation, the model we used here reasonably captures the observed PDO pattern with 10–20 year and 20–50 year periods.

In SOWH experiment, we find that in response to freshening over the Antarctic Ocean, the 20–50 year magnitude of the PDO is weakened and shifted toward high-frequency. However, the magnitudes of 10–20 year variability are slightly reinforced. One main reason is likely that freshening over the Antarctic Ocean enhances the ocean stratification in North Pacific through a deep-sea adjustment process and then leads to the acceleration of the first-mode baroclinic Rossby wave, the primary memory for PDO in the model, as a result of which the multidecadal magnitudes of the PDO are suppressed (20–50 year period). Also, the analysis of the upper-ocean heat budget reveals a dominant role of the anomalous meridional advection, heat flux and ocean mixing in the generation of decadal SST anomalies over the North Pacific.

Latif and Barnett^[25,26] propose that PDO may arise from an instability of the coupled ocean-atmosphere system over the North Pacific, so we calculated the air-sea coupling coefficient in the Tropical and North Pacific using the method created by Frankignoul and Kestenare^[68], and the results show that the air-sea coupling was weakened in both areas after freshening over the Antarctic Ocean. However, considering the complicity of the air-sea coupled system, the changes in the air-sea coupling need to be demonstrated further.

Although processes have been made to understand the impact of freshening over the Southern Ocean on PDO, some questions are still inclusive. For instance, our study is mainly based on one particular model, can we draw the same conclusion by using multi-model ensembles? Moreover, here freshwater flux was added uniformly to the south of 60°S as a virtual salt flux to represent the melting of Antarctic ice. A more realistic treatment that considers the effect of Freshwater flux (FWF) on the vertical velocity, oceanic temperature, and surface buoyancy flux should be used. Previous studies also showed that model resolution has an impact of the simulation results^[69], it will be interesting to see if a higher resolution model will provide the same result. We will explore these questions in our future work.

Acknowledgments

I gratefully acknowledge funding from the Japan Society for the Promotion of Science (JSPS) KAKENHI (grant JP19H05703). Discussions with Dr. Mao and Huang Ke also improved the manuscript significantly.

Data sets used in this study can be found at the following websites: HadISST: <https://www.metoffice.gov.uk/hadobs/hadisst/>; The monthly mean geopotential height data from NCAR/NCEP Reanalysis: <https://psl.noaa.gov/data/gridded/data.ncep.reanalysis.pressure.html>.

Conflict of interest

The author declares no conflict of interest.

References

1. Kanfoush SL, Hodell DA, Charles CD, et al. Millennial-scale instability of the Antarctic ice sheet during the last glaciation. *Science* 2000; 288(5472): 1815–1818. doi: 10.1126/science.288.5472.1815
2. Huang E, Tian J. Ice melt-water events and abrupt climate change during the last deglaciation. *Chinese Science Bulletin* 2008; 53: 1437–1447.
3. Doake CSM, Corr HFJ, Rott H, et al. Breakup and conditions for stability of the northern Larsen Ice Shelf, Antarctica. *Nature* 1998; 391: 778–780. doi: 10.1038/35832
4. Rignot E, Bamber JL, van den Broeke MR, et al. Recent Antarctic ice mass loss from radar interferometry and regional climate modelling. *Nature Geoscience* 2008; 1: 106–110. doi: 10.1038/ngeo102
5. Velicogna I, Sutterley TC, van den Broeke MR. Regional acceleration in ice mass loss from Greenland and Antarctica using GRACE time-variable gravity data. *Geophysical Research Letters* 2014; 119: 8130–8137. doi: 10.1002/2014GL061052
6. Rignot E, Mouginot J, Scheuchl B, et al. Four decades of Antarctic Ice Sheet mass balance from 1979–2017. *Environmental Sciences* 2019; 116(4): 1095–1103. doi: 10.1073/pnas.1812883116
7. Ma H, Wu L, Li Z. Impact of freshening over the Southern Ocean on ENSO. *Atmospheric Science Letters* 2013; 14(1): 28–33. doi: 10.1002/asl2.410
8. Ma H, Li Z, Feng T, Liu C. Impacts of freshwater forcing over the Southern Ocean on Southern Annual Mode (Chinese). *Journal of Meteorology and Environment* 2015; 31: 81–88.
9. Zhi H, Zhang RH, Lin P, Wang L. Quantitative analysis of the feedback induced by the freshwater flux in the tropical Pacific using CMIP5. *Advances in Atmospheric Sciences* 2015; 32(10): 1341–1353. doi: 10.1007/s00376-015-5064-0
10. Zhi H, Zhang RH, Lin P, Wang L. Simulation of salinity variability and the related freshwater flux forcing in the tropical Pacific: An evaluation using the Beijing normal university earth system model (BNU-ESM). *Advances in Atmospheric Science* 2015; 32(11): 1551–1564. doi: 10.1007/s00376-015-4240-6
11. Bakker P, Prange M. Response of the intertropical convergence zone to Antarctic ice sheet melt. *Geophysical Research Letter* 2018; 45: 8673–8680. doi: 10.1029/2018GL078659
12. Trenberth KE, Hurrell JW. Decadal atmosphere-ocean variations in the Pacific. *Climate Dynamics* 1994; 9(6): 303–319. doi: 10.1007/BF00204745
13. Mantua NJ, Hare SR, Zhang Y, et al. A Pacific interdecadal climate oscillation with impacts on salmon production. *Bulletin of the American Meteorological Society* 1997; 78(6): 1069–1080. doi: 10.1175/1520-0477(1997)078%3C1069:APICOW%3E2.0.CO;2
14. Minobe S. Resonance in bidecadal and pentadecadal climate oscillations over the North Pacific: Role in climatic regime shifts. *Geophysical Research Letters* 1999; 26(7): 855–858. doi: 10.1029/1999GL900119
15. Chhak KC, Lorenzo ED, Schneider N, Cummins PF. Forcing of low-frequency ocean variability in the Northeast Pacific. *Journal of Climate* 2009; 22(5): 1255–1276. doi: 10.1175/2008JCLI2639.1
16. Wallace JM, Gutzler DS. Teleconnections in the geopotential height field during the Northern Hemisphere winter. *Monthly Weather Review* 1981; 109: 784–812. doi: 10.1175/1520-0493(1981)109<0784:TITGHF>2.0.CO;2
17. Kwon YO, Deser C. North Pacific decadal variability in the Community Climate System model version 2. *Journal of Climate* 2007; 20(11): 2416–2433. doi: 10.1175/JCLI4103.1
18. Schneider N, Miller AJ, Pierce DW. Anatomy of North Pacific decadal variability. *Journal of Climate* 2002; 15(6): 586–605. doi: 10.1175/1520-0442(2002)015<0586:AONPDV>2.0.CO;2
19. Wu L, Liu Z, Gallimore R, et al. Pacific decadal variability: The tropical Pacific mode and the North Pacific mode. *Journal of Climate* 2003; 16(8): 1101–1120. doi: 10.1175/1520-0442(2003)16%3C1101:PDVTTP%3E2.0.CO;2
20. Ramos RD, Goodkin NF, Siringan FP, Hughen KA. Coral records of temperature and salinity in the Tropical Western Pacific reveal influence of the Pacific Decadal Oscillation since the late nineteenth century. *Paleoceanography and Paleoclimatology* 2019; 34(8): 1344–1358. doi: 10.1029/2019PA003684
21. Byrne SM, Merrifield MA, Carter ML, et al. Southern California winter precipitation variability reflected in 100-year ocean salinity record. *Communications Earth & Environment* 2023; 4(1): 143. doi: 10.1038/s43247-023-00803-8
22. Jyoti J, Swapna P, Krishnan R, Naidu CV. Pacific modulation of accelerated south Indian Ocean sea level rise during the early 21st Century. *Climate Dynamics* 2019; 53: 4413–4432. doi: 10.1007/s00382-019-04795-0
23. Miller AJ, Schneider N. Interdecadal climate regime dynamics in the North Pacific Ocean: Theories, observations and ecosystem impacts. *Progress in Oceanography* 2000; 47(2): 355–379. doi: 10.1016/S0079-6611(00)00044-6
24. Gu DF, Philander SGH. Interdecadal climate fluctuations that depend on exchanges between the tropics and extratropics. *Science* 1997; 275(5301): 805–807. doi: 10.1126/science.275.5301.805
25. Latif M, Barnett TP. Causes of decadal climate variability over the North Pacific and North America. *Science* 1994; 266(5185): 634–637. doi: 10.1126/science.266.5185.634

26. Latif M, Barnett TP. Decadal climate variability over the North Pacific and North America: Dynamics and predictability. *Journal of Climate* 1996; 9(10): 2407–2423. doi: 10.1175/1520-0442(1996)009%3C2407:DCVOTN%3E2.0.CO;2
27. Fang C. *The Effect of Global Warming on North Pacific Decadal Variability and the Possible Mechanism* [PhD thesis]. Ocean University of China; 2010.
28. Rashid HA, Power SB, Knight JR. Impact of multidecadal fluctuations in the Atlantic thermohaline circulation on Indo-Pacific climate variability in a coupled GCM. *Journal of Climate* 2010; 23: 4038–4044. doi: 10.1175/2010JCLI3430.1
29. Liu Z. Dynamics of interdecadal climate variability: A historical perspective. *Journal of Climate* 2012; 25(6): 1963–1995. doi: 10.1175/2011JCLI3980.1
30. Newman M, Alexander MA, Ault TR, et al. The Pacific Decadal Oscillation, revisited. *Journal of Climate* 2016; 29(12): 4399–4427. doi: 10.1175/jcli-d-15-0508.1
31. Liu Z, Di Lorenzo E. Mechanisms and predictability of Pacific decadal variability. *Current Climate Change Reports* 2018. doi: 10.1007/s40641-018-0090-5
32. Power S, Lengaigne M, Capotondi A, et al. Decadal climate variability in the tropical Pacific: Characteristics, causes, predictability and prospects. *Science* 2021; 374(6563): eaay9165. doi: 10.1126/science.aay9165
33. Frankignoul C, Hasselmann K. Stochastic climate models, Part II Application to sea-surface temperature anomalies and thermocline variability. *Tellus* 1977; 29(4): 289–305. doi: 10.3402/tellusa.v29i4.11362
34. Alexander MA, Penland C. Variability in a mixed layer ocean model driven by stochastic atmospheric forcing. *Journal of Climate* 1996; 9(10): 2424–2442. doi: 10.1175/1520-0442(1996)009%3C2424:VIAMLO%3E2.0.CO;2
35. Jin FF. A theory of interdecadal climate variability of the North Pacific ocean-atmosphere system. *Journal of Climate* 1997; 10(8): 1821–1835. doi: 10.1175/1520-0442(1997)010%3C1821:ATOICV%3E2.0.CO;2
36. Pierce DW, Barnett TP, Schneider N, et al. The role of ocean dynamics in producing decadal climate variability in the North Pacific. *Climate Dynamics* 2001; 18(1/2): 51–70. doi: 10.1007/s003820100158
37. Jacobs GA, Hurlburt HE, Kindle JC, et al. Decade-scale trans-Pacific propagation and warming effects of an El Niño anomaly. *Nature* 1994; 370(6488): 360–363. doi: 10.1038/370360a0
38. Graham NE. Decadal-scale climate variability in the tropical and North Pacific during the 1970s and 1980s observations and model results. *Climate Dynamics* 1994; 10(3): 135–162. doi: 10.1007/BF00210626
39. Alexander MA, Bladé I, Newman M, et al. The atmospheric bridge: The influence of ENSO teleconnections on air-sea interaction over the global oceans. *Journal of Climate* 2002; 15(16): 2205–2231. doi: 10.1175/1520-0442(2002)015<2205:TABTIO>2.0.CO;2
40. Miller AJ, Cayan DR, White BW. A westward-intensified decadal change in the North Pacific thermocline and gyre-scale circulation. *Journal of Climate* 1998; 11(12): 3112–3127. doi: 10.1175/1520-0442(1998)011%3C3112:AWIDCI%3E2.0.CO;2
41. Saravanan R, McWilliam JC. Advective ocean-atmosphere interaction: An analytical stochastic model with implications for decadal variability. *Journal of Climate* 1998; 11(2): 165–188. doi: 10.1175/1520-0442(1998)011<0165:AOAIAA>2.0.CO;2
42. Holland WR, Haidvogel DB. On the vacillation of an unstable baroclinic wave field in an eddy-resolving model of the oceanic general circulation. *Journal of Physical Oceanography* 1981; 11: 557–568. doi: 10.1175/1520-0485(1981)011<0557:OTVOAU>2.0.CO;2
43. Robertson AW. Interdecadal variability over the North Pacific in a multi-century climate simulation. *Climate Dynamics* 1996; 12: 227–241. doi: 10.1007/BF00219498
44. Guilderson TP, Schrag DP. Abrupt shift in subsurface temperatures in the tropical Pacific associated with changes in El Niño. *Science* 1998; 281(5374): 240–243. doi: 10.1126/science.281.5374.240
45. Liu Z, Zhang RH. Propagation and mechanism of decadal upper-ocean variability in the North Pacific. *Geophysical Research Letters* 1999; 26(6): 739–742. doi: 10.1029/1999GL900081
46. Zhang RH, Levitus S. Structure and cycle of decadal variability of upper ocean temperature in the North Pacific. *Journal of Climate* 1997; 10(4): 710–727. doi: 10.1175/1520-0442(1997)010<0710:SACODV>2.0.CO;2
47. Zhang RH, Rothstein LM, Busalacchi AJ. Origin of upper-ocean warming and El Niño change on decadal time scales in the tropical Pacific Ocean. *Nature* 1998; 391(6670): 879–883. doi: 10.1038/36081
48. Zhang RH, Rothstein LM, Busalacchi AJ. Interannual and decadal variability of the subsurface thermal structure in the Pacific Ocean: 1961–90. *Climate Dynamics* 1999; 15(10): 703–717. doi: 10.1007/s003820050311
49. Watanabe M, Kimoto M. Behavior of midlatitude decadal oscillations in a simple atmosphere-ocean system. *Journal of the Meteorological Society of Japan* 2000; 78(4): 441–460. doi: 10.2151/jmsj1965.78.4_441
50. Giese BS, Urizar SC, Fučkar NS. Southern Hemisphere origins of the 1976 climate shift. *Geophysical Research Letters* 2002; 29(2): 1014. doi: 10.1029/2001GL013268
51. Huang B, Mehta VM. Response of the Pacific and Atlantic oceans to interannual variations in net atmospheric freshwater. *Journal of Geophysical Research Atmospheres* 2005; 110(C8): C08008. doi: 10.1029/2004JC002830
52. Kang SM, Held IM, Frierson DMW, Zhao M. The response of the ITCZ to extratropical thermal forcing: Idealized slab-ocean experiments with a GCM. *Journal of Climate* 2008; 21(14): 3521–3532. doi: 10.1175/2007JCLI2146.1

53. Luo Y, Rothstein LM, Zhang RH, Busalacchi AJ. On the connection between South Pacific subtropical spiciness anomalies and decadal equatorial variability in an ocean general circulation model. *Journal of Geophysical Research Oceans* 2005; 110(C10): C10002. doi: 10.1029/2004JC002655
54. Luo Y, Rothstein LM, Zhang RH. Response of Pacific subtropical-tropical thermocline water pathways and transports to global warming. *Geophysical Research Letters* 2009; 36(4): L04601. doi: 10.1029/2008GL036705
55. Kay JE, Wall C, Yettella V, et al. Global climate impacts of fixing the Southern Ocean shortwave radiation bias in the Community Earth System Model (CESM). *Journal of Climate* 2016; 29(12): 4617–4636.
56. Jacob R. *Low Frequency Variability in a Simulated Atmosphere-Ocean System* [PhD thesis]. University of Wisconsin-Madison; 1997. 155p.
57. Liu Z, Kutzbach J, Wu L. Modeling climate shift of El Niño variability in the Holocene. *Geophysical Research Letters* 2000; 27(15): 2265–2268. doi: 10.1029/2000GL011452
58. Wu L, Liu Z. Decadal variability in the North Pacific: The eastern North Pacific mode. *Journal of Climate* 2003; 16(19): 3111–3131. doi: 10.1175/1520-0442(2003)016<3111:DVITNP>2.0.CO;2
59. Wu L, Liu Z. North Atlantic decadal variability: Air-sea coupling, oceanic memory, and potential northern hemisphere resonance. *Journal of Climate* 2005; 18(2): 331–349. doi: 10.1175/JCLI-3264.1
60. Rayner NA, Parker DE, Horton EB, et al. Global analyses of sea surface temperature, sea ice, and night marine air temperature since the late nineteenth century. *Journal of Geophysical Research* 2003; 108(D14): 4407. doi: 10.1029/2002JD002670
61. Huang RX. Real freshwater flux as a natural boundary condition for the salinity balance and thermohaline circulation forced by evaporation and precipitation. *Journal of Physical Oceanography* 1993; 23(11): 2428–2446. doi: 10.1175/1520-0485(1993)023<2428:RFFAAN>3E2.0.CO;2
62. Griffies SM, Pacanowski RC, Schmidt M, Balaji V. Tracer conservation with an explicit free surface method for z-coordinate ocean models. *Monthly Weather Review* 2001; 129(5): 1081–1098. doi: 10.1175/1520-0493(2001)129<1081:TCWAEF>3E2.0.CO;2
63. Kang X, Zhang RH, Wang G. Effects of different freshwater flux representations in an ocean general circulation model of the tropical Pacific. *Science Bulletin* 2007; 62(5): 345–351. doi: 10.1016/j.scib.2017.02.002
64. Ma H, Wu L. Global teleconnections in response to freshening over the Antarctic Ocean. *Journal of Climate* 2011; 24: 1071–1088. doi: 10.1175/2010JCLI3634.1
65. Yang Y, Wu L, Fang C. Will global warming suppress North Atlantic tripole decadal variability? *Journal of Climate* 2012; 25(6): 2040–2055. doi: 10.1175/JCLI-D-11-00164.1
66. Chelton DB, deSzoeko RA, Schlax MG, et al. Geographical variability of the first baroclinic Rossby radius of deformation. *Journal of Climate* 1998; 28(3): 433–460. doi: 10.1175/1520-0485(1998)028<0433:GVOTFB>3E2.0.CO;2
67. Liu Z, Alexander M. Atmospheric bridge, oceanic tunnel, and global climatic teleconnections. *Reviews of Geophysics* 2007; 45: RG2005. doi: 10.1029/2005RG000172
68. Frankignoul C, Kestenare E. The surface heat flux feedback. Part I: Estimates from observations in the Atlantic and the North Pacific. *Climate Dynamics* 2002; 19(8): 633–647. doi: 10.1007/s00382-002-0252-x
69. Liu J, Yuan C, Luo JJ. Impacts of model resolution on responses of western North Pacific tropical cyclones to ENSO in the HighResMIP-PRIMAVERA ensemble. *Frontier in Earth Science* 2023; 11: 1169885. doi: 10.3389/feart.2023.1169885